Invited Paper

Infrared photonic to plasmonic couplers using spray deposited conductive metal oxides

Justin W. Cleary*[1], Ricky Gibson[1,2], Evan M. Smith[1,3], Shiva Vangala[1,4], Isaiah O. Oladeji[5], Farnood Khalilzadeh-Rezaie[6], Kevin Leedy[1], and Robert E. Peale[6]

[1]Air Force Research Laboratory, Sensors Directorate, Wright-Patterson AFB, OH 45433, USA
[2]University of Dayton Research Institute, Dayton, OH 45469, USA
[3]KBRWyle Laboratories, Inc., Dayton, OH 45431, USA
[4]Azimuth Corporation, Dayton, OH 45431, USA
[5]SISOM Thin Films LLC, Orlando, FL 32805, USA
[6]Department of Physics, University of Central Florida, Orlando, FL 32816, USA

Abstract

In recent years, infrared plasmonics has turned towards materials that are wavelength and application tailorable, and which are geared towards CMOS processing. The transparent conductive oxides are very favorable towards infrared plasmonic applications for a number of reasons, one of which being the natural visible transparency due to their relatively large bandgap. Fluorine-doped tin oxide (FTO) is one such transparent and doping-tunable material that in addition is low cost due to spray deposition techniques that result in perfectly conformal coatings. In this work, a deposition recipe that gives high free carrier concentration was used to fabricate structures for demonstration of surface plasmon excitation. 1D gratings with a range of structural parameters were etched in silicon. Then the gratings were conformally coated with FTO by aqueous spray deposition. Excitation of surface plasmon polaritons (SPP) at mid- and long- wave infrared wavelengths on these gratings was demonstrated. The observed (SPP) excitation resonances agree will with analytical excitation calculations and numerical simulations. We show that grating heights of ~10-15% of the wavelength are optimum for achieving the strongest sharpest coupling to plasmonic resonances in the mid- and long-wave infrared. The presented results are compared with similar etched silicon gratings coated with Ga-doped ZnO (GZO). The dominant difference between our FTO and GZO measurements is the free carrier concentration. The useful wavelength range is predicted for FTO based plasmonics and compared with other plasmonic host materials. The work presented here could play a key role in novel decreased-cost detectors, filters, and on-chip optoelectronics.

Keywords: transparent oxides, plasmonics, infrared, optical materials, conductors, spray deposited

*Corresponding Author: Justin.Cleary.1@us.af.mil

1. INTRODUCTION

Surface plasmon polaritons (SPP) have enabled label-free biosensing for many years[1-3]. More recently, SPP's at longer infrared wavelengths have been have been considered for chemical sensing, filters, IR detectors, solar cells, on-chip interconnects, and modulators[4-6]. This has motivated investigation of new SPP host materials that have infrared plasma frequencies. There has been considerable focus on transparent conductive oxides (TCO), metal nitrides, semiconductors, and alloys between metals and Group IV materials[4-6]. We have specifically emphasized the fluorine-doped tin-oxide, a TCO with a number of significant benefits.

Oxide-based Materials and Devices VIII, edited by Ferechteh H. Teherani, David C. Look, David J. Rogers, Proc. of SPIE Vol. 10105, 101050E · © 2017 SPIE
CCC code: 0277-786X/17/$18 · doi: 10.1117/12.2254315

Fluorine-doped tin oxide (SnO_2:F or FTO) has high conductivity, which can be tailored by both doping and conditions of deposition. FTO uses low-cost and environmentally benign elements, especially in comparison to the well-established indium tin oxide. Our approach is an aqueous spray method, which allows low cost, large-area, coating via heterogeneous chemical reaction at surface nucleation sites. The dense strongly adherent nano-crystalline thin films are perfectly conformal. The method is low cost because no vacuum processes are used. We recently presented a comprehensive study of optoelectronic film properties as a function of growth conditions and doping[7]. The highest free carrier concentration achieved was 5 x 10^{20} cm^{-3}, which gives a plasma frequency that corresponds to a free space wavelength of 2 μm. Plasmonics in the mid-wavelength infrared (MWIR, 3-5 μm wavelength) and the long-wavelength infrared (LWIR, 8-12 μm wavelength) are enabled by our ability to deposit different FTO films with plasma-frequencies that span theses ranges. In this paper, we investigate highly conductive FTO as an infrared SPP host. Previous works have calculated FTO near-infrared to MWIR attenuated total reflection based[8] and preliminary LWIR grating based coupling[9] of photons to surface plasmons. Our approach is to study photon to plasmon excitation resonances on FTO lamellar grating couplers with varying physical parameters. Results are compared with those for the TCO Ga-doped zinc oxide (GZO) deposited by a more traditional vacuum process.

2. FABRICATION AND CHARACTERIZATION

FTO films were deposited on high resistivity silicon coated with a 10 nm hydrophilic SiO_2 layer. FTO was then deposited via SPEED (Streaming Process for Electrodeless Electrochemical Deposition). Details on the chemistry can be found in Ref. 10. These substrates were preheated to 480 °C. The F/Sn ratio in the precursor solution was 15%, which was shown to give free carrier concentration[7] ~ 5x10^{20} cm^{-3}. GZO films were deposited by Pulse Laser Deposition (PLD). The PLD targets were nominally 0.5 % and 3% weight Ga_2O_3. These have free carrier concentrations of ~ 2 x 10^{20} and 1 x 10^{21} cm^{-3} (see Refs. 11 and 12 respectively).

Lamellar grating couplers were fabricated by deep-reactive ion etching of silicon, followed by 10 nm SiO_2 deposition and ~600 nm of FTO spray deposition. GZO films of ~1 μm thickness were deposited on similarly etched silicon substrates. The considered thicknesses are at least twice the infrared penetration depth in each case. Etched silicon grating heights of 0.51, 0.84, 1.49, and 1.83 μm were determined by cross-sectional scanning electron microscopy (SEM). Figure 1 presents two examples, which demonstrate that the films are conformal and rather uniform. Some of the dense nanocrystalline structure is also evident. Gratings with periods 7.5, 10, 15, and 20 μm and nominal 50% duty cycle were fabricated. SEM images (Figure 2) show the duty cycle of the grating bars is less than 50% due to over-etching, which is only partly compensated by infilling with FTO. This deviation from 50% duty is especially prominent for the small-period gratings.

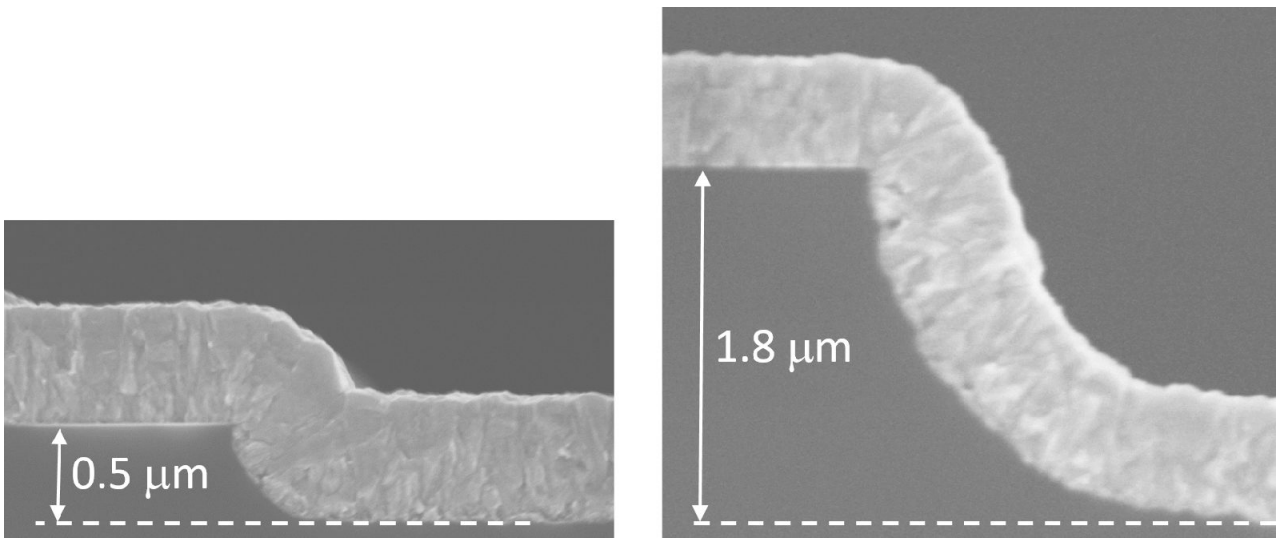

Figure 1: SEM cross sections showing the 0.6 μm thick FTO spray deposited on top of etched silicon gratings. Grating heights of 0.5 (left) and 1.8 μm (right) are shown.

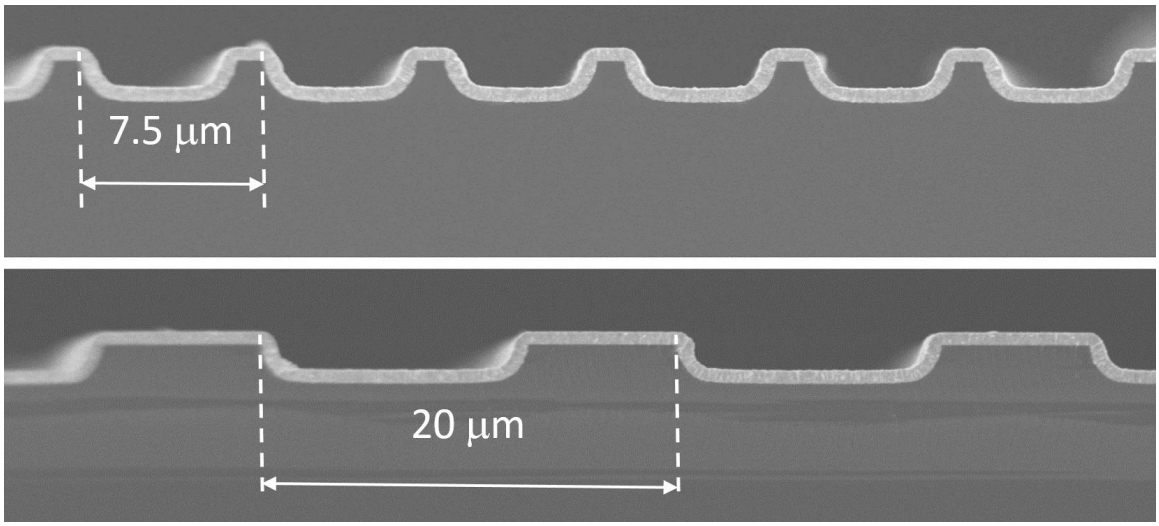

Figure 2: SEM cross sections showing the 0.6 μm thick FTO spray deposited on top of etched silicon gratings. Grating periods of 7.5 (top) and 20 μm (bottom) are shown.

Infrared ellipsometry (J.A. Woollam IR-VASE) determined the optical constants of the unstructured films. These constants were used in analytical calculations and electromagnetic simulations (Lumerical FDTD). Film thicknesses were determined from SEM cross sections. The photonic-to-plasmonic excitation resonances on grating couplers were characterized via angular-dependent reflection measurements using a computer-controlled rotation stage, MWIR and LWIR quantum cascade lasers (Daylight Solutions) and an MCT detector. The light was TM polarized as required for SPP excitation on gratings.

3. GRATING HEIGHT AND PERIOD DEPENDENCE

Surface plasmon resonances on conducting gratings satisfy[13]

$$\mathrm{Re}\left[\sqrt{\frac{\varepsilon_d\,\varepsilon_c}{\varepsilon_d+\varepsilon_c}}\right] sign(m) = \sin(\theta) + \frac{m\lambda}{P}, \tag{1}$$

where λ is the free space wavelength, P is the grating period, m is an integer of either sign, θ is the angle of incidence, and ε_d and ε_c are the complex permittivities of the dielectric (air in our case) and conductor. Eq. (1) was used to determine the expected resonance angles for given gratings. Analytic expressions for the full resonance line shape as a function of grating height, shape, and duty are quite difficult to use[13-14], so that we rely here on numerical calculations using Lumerical FDTD software.

Figure 3 presents reflectance as a function of θ at λ = 9.25 μm for gratings with different periods and heights. The resonance angles calculated using Eq. (1) are indicated by symbols and labeled by their m values. We note that since the gratings have nominally a 50% duty cycle, only odd order modes are allowed since only those Fourier harmonics are present with respect to the grating profile[14]. We note however, that as the period decreases the etched gratings had slightly less than 50% duty cycle which result in some cases of weak even orders being present. Even orders with noticeable features present in the data are found for P = 20 μm (m = 4, θ = 57.6°) and P = 10 μm (m = 2, θ = 57.6°). For the 20 and 15 μm periods, the 1 and -3 resonances dominate, but for 10 and 7.5 μm periods these are outside our angular range. The grating height 0.84 μm gives the deepest and sharpest resonances. We previously noted for silver gratings[13] that optimum coupling occurred for grating heights 10-15% of the wavelength, which is confirmed here even though the optical constants for FTO are quite different.

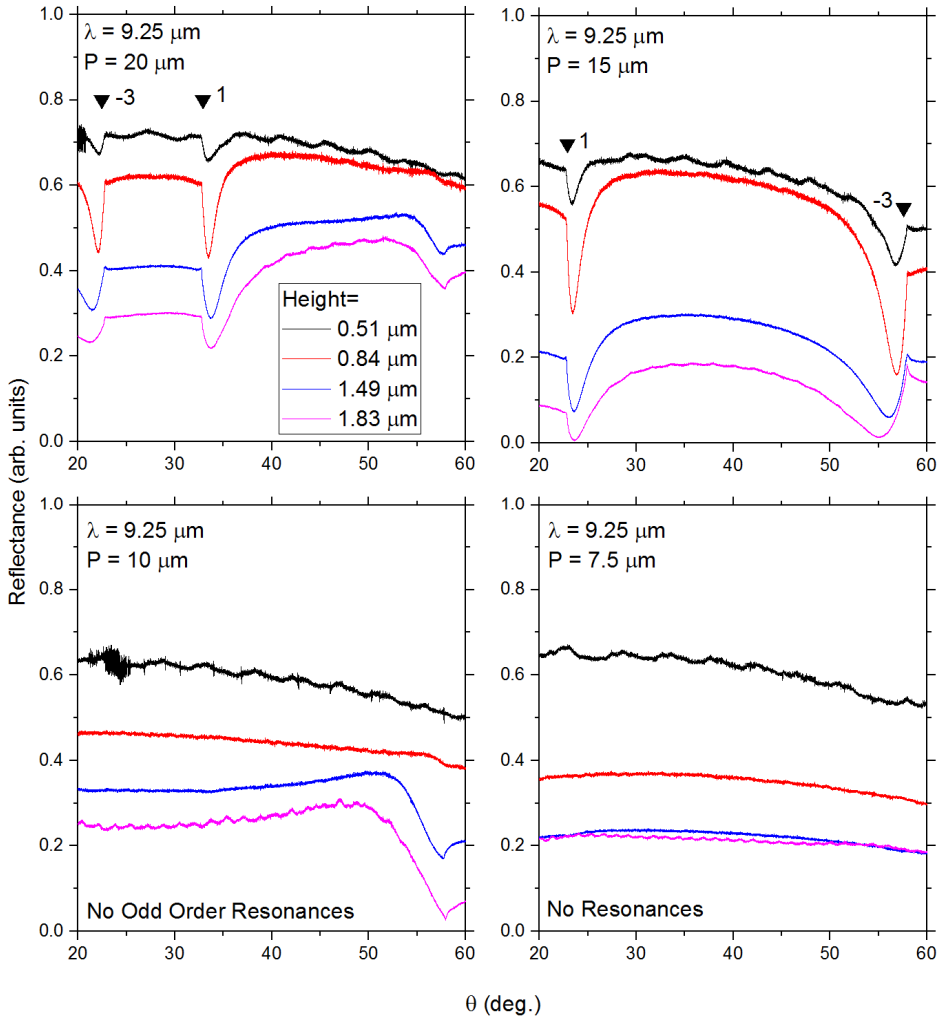

Figure 3: Reflectance as a function of angle for grating structures with multiple heights at λ = 9.25 μm. Clockwise from top-left is for grating periods of 20, 15, 10, and 7.5 μm.

Figure 4 presents reflectance for the same gratings at λ = 4.71 μm. As Fig. 3, odd resonant orders dominate. In contrast to Fig. 3, the m = 1 resonance is observed for all grating periods. The higher order resonances move very rapidly through the angular range as the period is changed. The 0.84 μm grating height still gives the strongest resonances for the two larger periods. As the period decreases however, the 0.51 μm grating height shows resonances increasing in strength and becoming comparable to and even stronger than the taller grating. It is possible that a more optimum grating height exists between the two investigated here, which is still consistent with the optimum height being 10-15% of the wavelength[13]. We note, as with Fig. 3, weak even resonance orders are observable due to the duty cycle being slightly decreased from 50%. Those even orders are for P = 20 μm (m = -6, θ = 23.1°, and m = 2, θ = 33.3°), and P = 15 μm (m = -6, θ = 59.7°, and m = 2, θ = 23.1°).

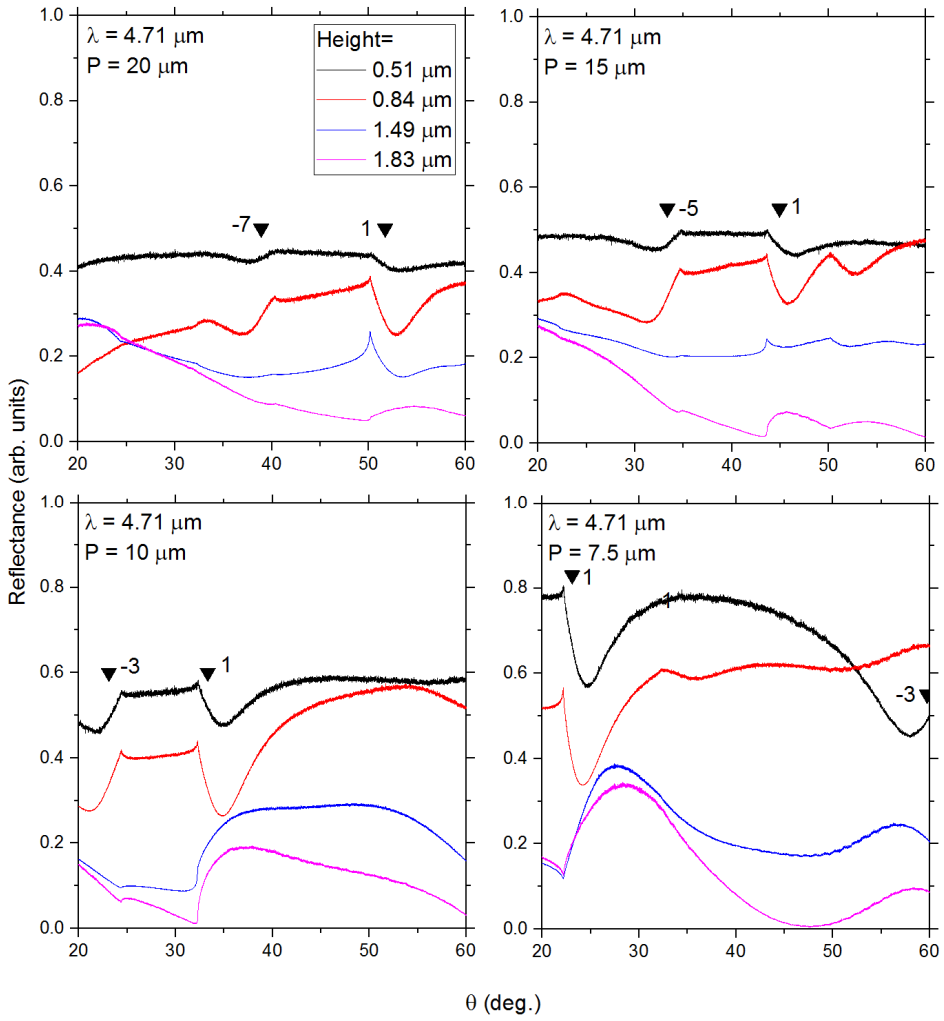

Figure 4: Reflectance as a function of angle for grating structures with multiple heights at λ = 4.71 μm. Clockwise from top-left is for grating periods of 20, 15, 10, and 7.5 μm.

4. FTO AND GZO COMPARISON

We now compare results for FTO and GZO gratings. The latter have been the subject of a number of studies already[4-6]. Figure 5 compares their complex permittivity spectra. The zero crossing of real part of the permittivity ε' for FTO occurs between the values for the two GZO films with different carrier concentrations. The imaginary component, ε", of FTO similarly falls between that of the GZO with differing carrier concentrations. The losses are predominately attributed to free carrier absorption in both, as opposed to lattice effects, so there is no reason to prefer GZO over FTO on basis of loss.

Figure 5 also presents numerically-calculated angle-dependent reflectance spectra based on the measured optical constants. The reflectance here however is taken in the near-field which sums over diffracted orders while the experiment is far-field and is limited to specular reflection. Moreover, the simulations assume 50% silicon grating duty cycle with conformal 0.6 μm thick TCO films. The films are optically thick so the material can in principal can be infinitely thick. However we implemented the film as a way to more accurately represent deviations from 50% duty cycle from the addition of the conformal coating. The FTO simulated resonances qualitatively match the experimental result, which is also presented in Fig. 5. The 0.5% GZO gives relatively broad and shallow resonances compared with the higher concentration sample. Figure that SPP coupling resonances for FTO compare well with those for the more standard GZO when carrier concentrations are similar.

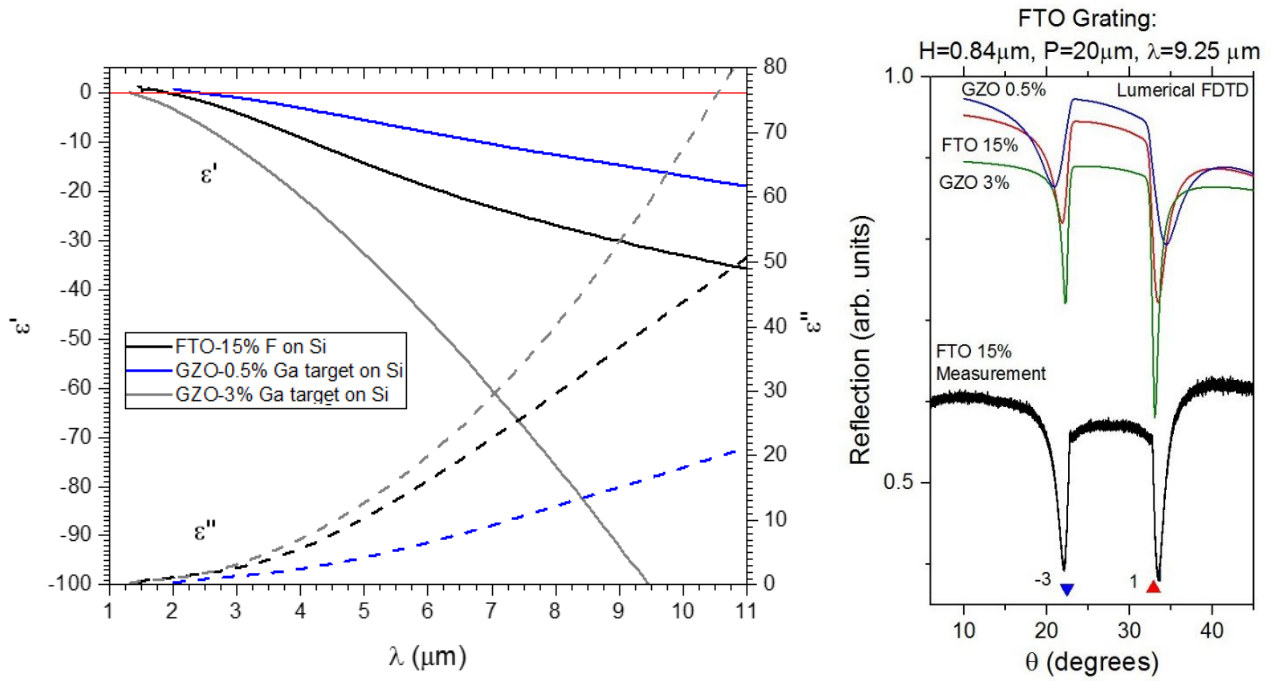

Figure 5: (left) Complex permittivity data for FTO and GZO for multiple nominal doping ratios. (right) Lumerical FDTD simulations and demonstrating reflectance of photonic to plasmonic grating couplers using the same TCO materials in conjunction with measured FTO data.

SPP intensity propagation length is calculated according to[15]

$$L_z = \left[\frac{\omega}{c} \mathrm{Im} \sqrt{\frac{\varepsilon_d \, \varepsilon_c}{\varepsilon_d + \varepsilon_c}} \right], \tag{2}$$

and the field penetration depth is

$$L_{d,c} = \left[\frac{\omega}{c} \mathrm{Re} \sqrt{\frac{-\varepsilon^2{}_{d,c}}{\varepsilon_d + \varepsilon_c}} \right]^{-1} . \tag{3}$$

The wavelength range that is useful for plasmonic applications range can be defined by the criteria[16] that the characteristic propagation length for SPP intensity must be at minimum two wavelengths and that the field penetration depth into the dielectric (air) is no more than three wavelengths, i.e.

$$L_z(\lambda_{low}) = 2\lambda_{low} \quad \text{and} \quad L_d(\lambda_{high}) = 3\lambda_{high} . \tag{4}$$

Figure 6 presents these ranges for several plasmonic hosts together with the zero crossings for ε'. These predictions show that the range for our FTO falls in between those for the two GZO samples. For all TCOs shown, the long wave limit extends beyond the LWIR range, so that the limiting factor is on the low wavelength side, which is due to propagation length. The metal silicides[17], and $PtGe_2$[18] are useful in the MWIR but not in the LWIR. Pt_2Ge_3[18] itself does appear useful throughout the MWIR and most of the LWIR, but unlike FTO this range cannot be adjusted. Doped-Si, on the other hand, can be tuned, and several studies have demonstrated its promise as a LWIR SPP host[19-21], but limits to

achievable free carrier concentration[21] confine it to plasmonic applications beyond ~4 μm wavelength. The advantages of optical transparency and spray deposition for FTO are sure to enable numerous application while restraining costs.

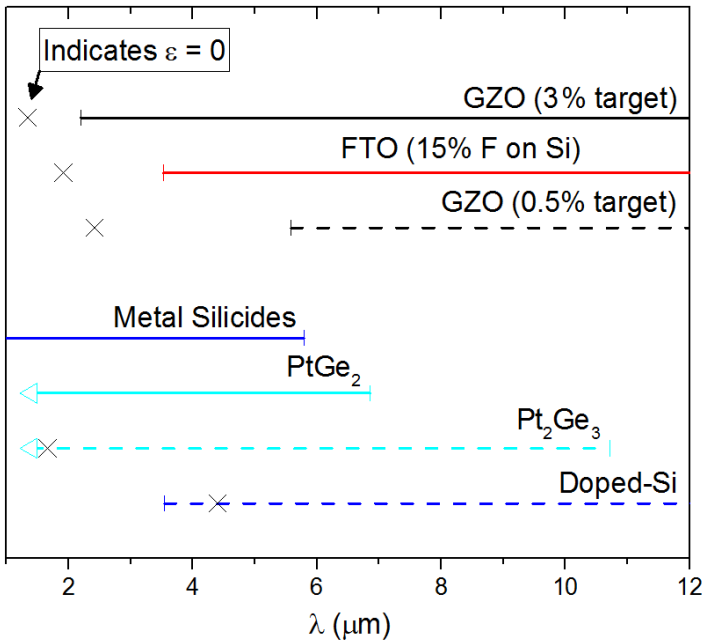

Figure 6: Predicted useful wavelength range for highly conductive FTO, GZO and several Group IV based materials[17-18,21].

5. SUMMARY

Fluorine-doped tin oxide was investigated as a surface plasmon polaritons host for MWIR and LWIR. Spray deposited films roughly 600 nm thick with free carrier concentrations of 5 x 10^{20} cm^{-3} have negative permittivities beyond ~2 μm wavelength, making them attractive for plasmonic applications at longer wavelengths. We fabricated FTO grating couplers and characterized their photon-to-plasmon excitation resonances grating couplers. Grating heights of ~10-15% of the wavelength proved optimum for achieving the strongest sharpest coupling resonances. Expanded analysis of FTO gratings for MWIR and LWIR plasmonics are in progress[22]. Comparison of FTO with GZO shows that the differences depend mainly on carrier concentration.

ACKNOWLEDGMENTS

AFRL authors were supported by Air Force Office of Scientific Research under AFOSR LRIR No. 15RYCOR162 (Program Officer Dr. Gernot Pomrenke). UCF authors acknowledge AFRL contract FA8650-16-C-1738. Author Peale acknowledges support for two summer visits to AFRL Sensors Directorate WPAFB.

REFERENCES

[1] Homola, J., "Present and future of surface plasmon resonance biosensors," Anal. Bioanal. Chem. 377, 528-539 (2003).
[2] Rich R. L. and Myszka, D. G., "Advances in surface plasmon resonance biosensor analysis," Curr. Opin. Biotech. 11, 54-61 (2000).
[3] Zhao, J., Zhang, X., Yonzon, C. R., Haes, A. J. and Van Duyne, R. P., "Localized surface plasmon resonance biosensors," Nanomedicine 1, 219-228 (2006).
[4] Naik, G., Shalaev, V. M. and Boltasseva, A. "Alternative plasmonic materials: beyond gold and silver," Adv. Mater. 25, 3264-3294 (2013).
[5] Law, S., Podolskiy, V. and Wasserman, D. "Towards nano-scale photonics with micro-scale photonics; the opportunities and challenges of mid-infrared plasmonics," J. Nanophotonics, A 24, 103-130 (2013).
[6] Zhong, Y., Malagari, S. D., Hamilton, T. and Wasserman, D., "Review of mid-infrared plasmonic materials," J. Nanophotonics, 9(1), 093791 (2015).

[7] Peale, R. E., Smith, E., Abouelkahir, H., Oladeji, I. O., Vangala, S., Cooper, T., Grzybowski, G., Khalilzadeh-Rezaie, F., and Cleary, J. W. “Electrodynamic properties of aqueous spray deposited SnO2:F films for infrared plasmonics,” to be submitted to SPIE Optical Engineering (2017).
[8] Dominici, L., Michelotti, F., Brown, T. M., Reale, A. and Di Carlo, A. "Plasmon polaritons in the near infrared on fluorine doped tin oxide films," Opt. Express 17(12), 10155-10167 (2009).
[9] Khalilzadeh-Rezaie, F., Oladeji, I. O., Cleary, J. W., Nader, N., Nath, J., Rezadad, I. and Peale, R. E. "Fluorine-doped tin oxides for mid-infrared plasmonics," Opt. Mater. Express 5(10), 2184-2192 (2015).
[10] Khalilzadeh-Rezaie, F., Oladeji, I., Yusuf, G., Nath, J., Nader, N., Vangala, S., Cleary, J., Schoenfeld, W. and Peale, R. E., “Optical and electrical properties of tin oxide-base thin films prepared by streaming process for electrodeless electrochemical deposition,” Proc. MRS 1805, 2136423 (2015).
[11] Cleary, J. W., Nader, N., Leedy, K. D. and Soref, R., “Tunable short- to mid-infrared perfectly absorbing thin films utilizing conductive zinc oxide on metal,” Opt. Mat. Express 9, 1898-1909 (2015).
[12] Cleary, J. W., Snure, M. R., Leedy, K. D., Look, D. C., Eyink, K. and Tiwari, A., "Mid- to long-wavelength infrared surface plasmon properties in doped zinc oxides," Proc. SPIE 8545, 854504 (2012).
[13] Cleary, J. W., Peale, R. E., and Buchwald, W. R., “Long-wave infrared surface plasmon grating coupler,” Appl. Opt. 49, 3102-3110 (2010).
[14] Avrutsky, I., Smith, C. W., Cleary, J. W. and Hendrickson, J. R., “Resonant diffraction into symmetry-prohibited orders of metal gratings,” IEEE J. of Quantum Optics 51, 6600209 (2015).
[15] Raether, H. [Surface Plasmons on Smooth and Rough Surfaces and on Gratings] Springer, New York (1988).
[16] Soref, R., Peale, R. E. and Buchwald, W., “Longwave plasmonics on doped silicon and silicides,” Opt. Express 16, 6507-6514 (2008).
[17] Cleary, J. W., Peale, R. E., Shelton, D. J., Boreman, G. D., Smith, C. W., Ishigami, M., Soref, R., Drehman, A. and Buchwald, W.R., “IR permittivities for silicides and doped silicon,” J. Opt. Soc. Am. B 27, 730-734 (2010).
[18] Cleary, J. W., Streyer, W. H., Nader, N., Vangala, V., Avrutsky, I., Claflin, B., Hendrickson, J., Wasserman, D., Peale, R. E., Buchwald, W. R. and Soref, “Platinum germanides for mid- and long-wave infrared plasmonics,” Opt. Express 23,3316-3326 (2015).
[19] Shahzad, M., Medhi, G., Peale, R. E., Buchwald, W. R., Cleary, J. W., Soref, R., Boreman, G. D. and Edwards, O., “Infrared surface plasmons on heavily doped silicon,” J. Appl. Phys., 110, 123105 (2011).
[20] Ginn, J. C., Jarecki, Jr., R. L., Shaner, E. A., and Davids, R. S., “Infrared plasmons on heavily-doped silicon,” J. Appl. Phys. 110, 043110 (2011).
[21] Streyer, W., Law, S., Rooney, G., Jacobs, T. and Wasserman, D., "Strong absorption and selective emission from engineered metals with dielectric coatings," Opt. Express 21, 9113-9122 (2013).
[22] Gibson, R., Vangala, S., Oladeji, I. O., Smith, E., Khalizadeh-Resaie, F., Leedy, K., Peale, R. E. and Cleary, J. W., “Conformal spray deposited fluorine doped tin oxide for mid- and long-wave infrared plasmonics,” in preparation for Opt. Mat. Express (2017).